Accuracy of the cylinder approximation for susceptometric measurement of intravascular oxygen saturation versus numerical calculation of induced field

C. Li[1], M. C. Langham[1], J. F. Magland[1], C. L. Epstein[1,2], J. Wu[1], J. C. Gee[1], and F. W. Wehrli[1]

[1]Department of Radiology, University of Pennsylvania, Philadelphia, PA, United States, [2]Department of Mathematics, University of Pennsylvania, Philadelphia, PA, United States

Introduction MR susceptometry-based oximetry exploits the field shift of the water protons of intravascular blood relative to surrounding reference tissue for blood hemoglobin oxygen saturation (*HbO_2*) quantification (1, 2). The method has recently been applied to quantify peripheral vascular reactivity in patients with peripheral arterial disease (3) and cerebral metabolic rate of oxygen utilization (4). In these applications the femoral vein and superior sagittal sinus (SSS) have been modeled as long paramagnetic cylinders (3, 4). However, bifurcations, tapering, non-circular cross-section and curvature in the geometries of these vessels produce substantial deviation from a cylindrical geometry, which may lead to errors in *HbO_2* quantification. Here, we investigate the accuracy of the "long cylinder" approximation in MR susceptometry against numerical calculation based on 3D geometries of femoral vein and SSS obtained from segmented MR venograms. The cylinder approximation was validated by comparison between the pre-selected *HbO_2* (referred to as "actual") and *HbO_2* estimated from the simulated magnetic field by modeling the vessel as a tilted cylinder.

Methods ***MR image acquisition***: Axial multi-slice 2D TOF with tracking saturation (to suppress arterial blood signal) was used to image the femoral vein and SSS at 3T (Siemens TIM Trio). For the femoral vein, the scan parameters were: FOV = 160×160 mm^2 with 128 slices, voxel size = 0.63×0.63×1.5 mm^3 with 0.3 mm overlap between slices, TR = 33 ms, TE = 5.56 ms, FA = 60°. Scan parameters for the SSS were identical except: FOV= 210×210 mm^2 with 70 slices, voxel size = 0.55×0.55×1.5 mm^3.

Image post processing: The MR images were first resampled to isotropic voxel size of 0.5×0.5×0.5mm^3 by cubic-spline interpolation and then vessels were segmented by means of a level set algorithm. Since the femoral vein and SSS have high contrast with surrounding tissue in the venogram images, the region competition feature images can be easily obtained by thresholding the image intensities, which were then used to drive level set evolutions to generate 3D vessel geometries. All image processing was done in ITK-SNAP (6).

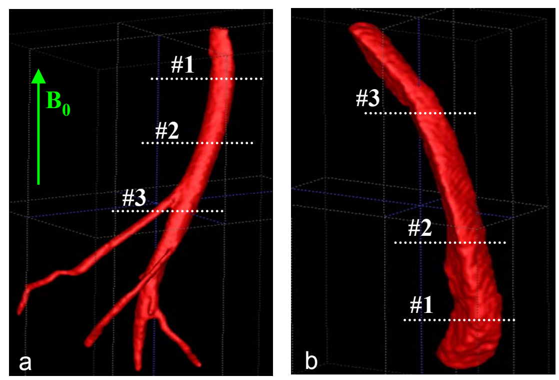

Fig.1 3D Renderings of (a) femoral vein and, (b) SSS.

Magnetic field calculation and HbO_2 estimation: From the segmented 3D binary images, 3D susceptibility maps were generated by assigning voxels classified as extravascular tissue a value of 0 while intravascular voxels were assigned a susceptibility value according to $\Delta\chi=\Delta\chi_{do}\text{Hct}\cdot(1\text{-}HbO_2)$, where $\Delta\chi_{do}$=4π·0.27ppm is the susceptibility difference between fully deoxygenated and fully oxygenated erythrocytes, *Hct* is the volume fraction of red blood cells in packed blood and *HbO_2* is the fraction of oxygenated hemoglobin. For *Hct* and *HbO_2*, typical values of 0.42 and 0.65 were used. The induced magnetic field of the 3D susceptibility distribution was then calculated using a perturbation method following Jenkinson et al (5) since $\Delta\chi$<<1. For each slice location %*HbO_2* was computed using the analytical long cylinder solution $\%HbO_2=[1-2\Delta B/(\Delta\chi_{do}(\cos^2\theta-1/3)Hct)]\times100$ (1, 2), where ΔB (in ppm) is the field difference between the intravascular blood and the surrounding reference tissue, θ is the local vessel tilt angle relative to the main field B_0 measured from the segmented images based on the coordinate of the vessel's centroid separated by approximate 5mm in B_0 direction. To evaluate the accuracy of the cylinder approximation, the estimated values of %*HbO_2* were compared with the "actual" %*HbO_2* values at various vessel locations.

Results 3D rendered venograms of femoral and SSS are shown in Fig. 1. Vessel geometries deviate substantially from circular cylinder geometry (e.g. bifurcation, tapering, non-circularity and curvature). The locations at which *HbO_2* was estimated are labeled in Fig.1. Field maps based on the numerical calculation (Fig 2a) and analytical solution (Fig 2b) at location #2 of femoral vein are in good agreement. The reference muscle tissue region is labeled in Fig 2a. Estimated %*HbO_2* based on the cylinder approximation are in good agreement with actual value at different locations for both veins (Table 1). Locations #1 in both vessels are nearly parallel to the main field but not circular (in particular the SSS is triangular) but the relative error in *HbO_2* is less than 3%. At the locations #2 both vessels are tilted ~30° relative to the main field, yet the error in *HbO_2* is within 5%. Even at the bifurcation (location #3 in a), the relative error is less than 7% (4% absolute *HbO_2*). The results for the SSS also indicate vessel circularity is not critical as previously found for tilt angle ≤ 30°.

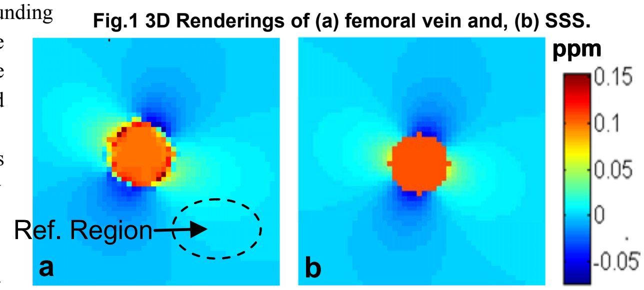

Fig.2 (a) Numerically calculated field and (b) analytical field of cylinder at location #2 of femoral vein (tilt angle 30°).

Table 1 Comparison between numerical calculation and "long cylinder" approximation

Location		*HbO_2* Actual (%)	*HbO_2* Estimated (%)	Relative Error (%)
Femoral vein	#1	65	67	3
	#2	65	68	4.6
	#3	65	61	6.2
SSS	#1	65	66	1.5
	#2	65	66	1.5
	#3	65	67	3

Conclusion The comparisons between "actual" and estimated *HbO_2* via cylinder approximation indicated that modeling femoral vein and SSS as "long cylinder" is valid in a large portion of these vessels. The simulation results also provide the guideline to choose a safe segment of the vessels to measure the *HbO_2* more accurately: the segment should be straight and nearly parallel to the main field.

Acknowledgements NIH Grants RO1-MH080892 and R21-HL088182

References 1.Haacke EM et al., Hum Brain Mapp1997;5:341-6 2. Fernandez-Seara MA et al., MRM2006;55:967-73; 3. Langham MC et al., MRM2009;62:333-40; 4. Jain V et al., JCBFM2010;30:1598-1607; 5. Jenkinson M et al., MRM2004;52:471-477; 6. Yushkevich PA et al., Neuroimage 2006, 31:1116-28.